

Incorporation of an Allene Unit into α -Pinene: Generation of the Cyclic Allene 2,7,7-Trimethylbicyclo[4.1.1]octa-2,3-diene and Its Dimerization

Akin Azizoğlu,^{†,‡} Recep Özen,^{†,§} Tuncer Hökelek,^{⊥,||} and Metin Balci^{*,†}

Department of Chemistry, Middle East Technical University, 06531 Ankara, Turkey, Department of Chemistry, Balıkesir University, 10100 Balıkesir, Turkey, Department of Chemistry, Mersin University, 33342 Mersin, Turkey, and Department of Physics, Hacettepe University, 06532 Ankara, Turkey

mbalci@metu.edu.tr

Received October 2, 2003

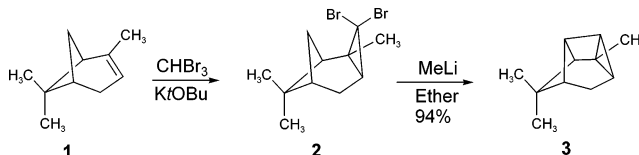
The reaction of ethereal methyllithium with 3,3-dibromo-2,7,7-trimethyl-tricyclo[4.1.1.0^{2,4}]octane (**2**) was investigated. The generated carbene **12** undergoes intramolecular C–H insertion to provide the tetracyclic hydrocarbon **3** and the bicyclic allene **15**, which undergoes [2+2] cyclodimerization. The structures of the formed allene dimers **16**, **17**, and **18** were elucidated by spectral means. The activation barriers for all possible C–H insertion products **3**, **13**, and **14** and the allene **15** were investigated by using density functional theory computations at the B3LYP/6-31G(d) level. It was found that the activation barriers for the formation of **3** and **15** (6.2 and 6.3 kcal mol⁻¹) are much lower than that for the insertion products **13** and **14** (17.5 and 12.6 kcal mol⁻¹), respectively. This prediction was completely in agreement with our experimental results.

Introduction

The synthesis of cyclic-strained allenes has been attracting more and more interest in the past few decades.¹ Besides the synthesis, these compounds have been the subject of several theoretical investigations.² Incorporation of an allene unit in small carbocyclic rings causes considerable deformation from the linear geometry, as the ring constraints exert torsion toward the planar rearrangement.³

From among the numerous synthetic approaches¹ to the cyclic allenes currently available, the conversion of 1,1-dihalocyclopropanes⁶ to the corresponding cyclic al-

SCHEME 1



lenes upon treatment with alkylolithium reagents^{3,7} discovered by Moore and co-workers⁴ and Skattebol⁵ has played the most important role.

This paper describes an investigation aimed at the incorporation of an allene unit into a natural product, being α -pinene, by using the above-mentioned method. It has been reported independently by Baird et al. and Waegell et al.⁸ in the literature that the reaction of dibromide **2** formed by the addition of dibromocarbene to α -pinene exclusively provides the insertion product **3** upon treatment with methyllithium in a 94% yield (Scheme 1). However, 2,7,7-trimethylbicyclo[4.1.1]octa-2,3-diene (**15**), whose allene bond is located in a seven-membered ring, was not observed.

The Doering–Moore–Skattebol method is the most efficient for the generation of 1,2-cyclohexadiene **5**,⁹ but

* To whom correspondence should be addressed.

[†] Middle East Technical University

[‡] Balıkesir University

[§] Mersin University

[⊥] Hacettepe University

^{||} To whom correspondence concerning the X-ray analysis should be sent.

(1) (a) Balci, M.; Taskesenligil, Y. In *Advances in Strained and Interesting Organic Molecules*; Halton, B., Ed.; JAI Press Inc: Stamford, CT, 2000; Vol. 8, pp 43–81. (b) Johnson, R. P. *Chem. Rev.* **1989**, *89*, 1111–1124.

(2) (a) Engels, B.; Schoneboom, J. C.; Munster, A. F.; Groetsch, S.; Christl, M. *J. Am. Chem. Soc.* **2002**, *124*, 287–297. (b) Nendel, M.; Tolbert, L. M.; Herring, L. A.; Islam, Md. N.; Houk, K. N. *J. Org. Chem.* **1999**, *64*, 976–983. (c) Angus, R. O., Jr.; Schmidt, M. W. *J. Am. Chem. Soc.* **1985**, *107*, 532–537. (d) Yavari, I.; Nori-Shargh, D.; Najafian, K. *J. Mol. Struct.: THEOCHEM* **1999**, *467*, 147–152.

(3) For very recent synthesis of some cyclic strained allenes see: (a) Ogawa, K.; Okazaki, T.; Kinoshita, T. *J. Org. Chem.* **2003**, *68*, 1579–1581. (b) Algi, F.; Özen, R.; Balci, M. *Tetrahedron Lett.* **2002**, *43*, 3129–3131. (c) Özen, R.; Balci, M. *Tetrahedron* **2002**, *58*, 3079–3083.

(4) (a) Moore, W. R.; Ward, H. R. *J. Org. Chem.* **1960**, *25*, 2073. (b) Moore, W. R.; King, B. J. *J. Org. Chem.* **1971**, *36*, 1877–1882.

(5) (a) Skattebol, L. *Tetrahedron Lett.* **1961**, 167–172. (b) Skattebol, L. *Acta Chem. Scand.* **1963**, *17*, 1683.

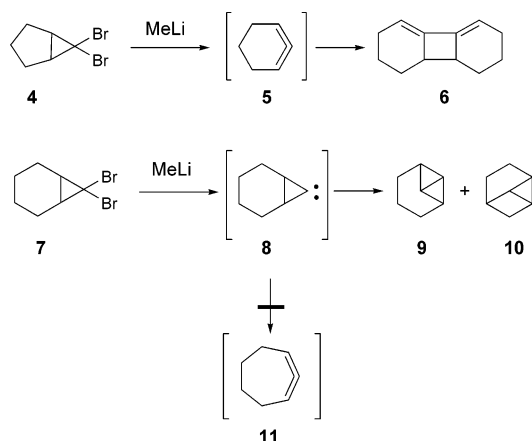
(6) (a) Sydnes, L. K. *Chem. Rev.* **2003**, *103*, 1133–1150. (b) Fedorynski, M. *Chem. Rev.* **2003**, *103*, 1099–1132.

(7) (a) Doering, W. v. E.; LaFlamme, P. M. *Tetrahedron* **1958**, *2*, 75–79. (b) Christl, M.; Groetsch, S.; Günther, K. *Angew. Chem., Int. Ed. Engl.* **2000**, *39*, 3261–3263. (c) Tolbert, M. L.; Islam, M. N.; Johnson, R. P.; Loisel, P. M.; Shakespeare, W. C. *J. Am. Chem. Soc.* **1990**, *112*, 6416–6417. (d) Christl, M.; Schreck, M. *Chem. Ber.* **1987**, *120*, 915–920. (e) Christl, M.; Braun, M. *Chem. Ber.* **1989**, *122*, 1939–1946. (f) Christl, M.; Braun, M.; Wagner, W. *Chem. Ber.* **1994**, *127*, 1137–1142.

(8) Baird, M. S.; Sadler, P.; Hatem, J.; Zahra, J.-P.; Waegell, B. *J. Chem. Soc., Chem. Commun.* **1979**, 452–453.

(9) Moore, W. R.; Moser, W. R. *J. Am. Chem. Soc.* **1970**, *92*, 5469–5474.

SCHEME 2



paradoxically, this method was not successful for the synthesis of 1,2-cycloheptadiene **11** (Scheme 2).^{4a,10,11} Hence, Schleyer et al. have focused on the ring opening of bicyclo[4.1.0]hept-7-ylidene (**8**)¹² by using density functional theory computations at the B3LYP/DZP and TZP levels.¹³

They found that the ring opening of **8** to **11** has an unusually high activation energy of 14.6 kcal/mol because of the unfavorable conformational changes in the cyclohexane moiety of **8** during the reaction. However, the activation barriers for intramolecular CH-insertions to yield highly strained hydrocarbons, tricyclo[4.1.0.0^{2,7}]heptane (**9**) and tricyclo[4.1.0.0^{3,7}]heptane (**10**), were found to be 6.4 and 9.1 kcal/mol, respectively. They concluded that the half-chair conformation of the cyclohexane moiety in **8** must change to a chair conformation during the reaction. To address the question of “why does 2,7,7-trimethyltricyclo[4.1.1.0^{2,4}]oct-3-ylidene (**12**) fail to provide allene **15**”, we studied the ring opening of **12** with DFT computations.

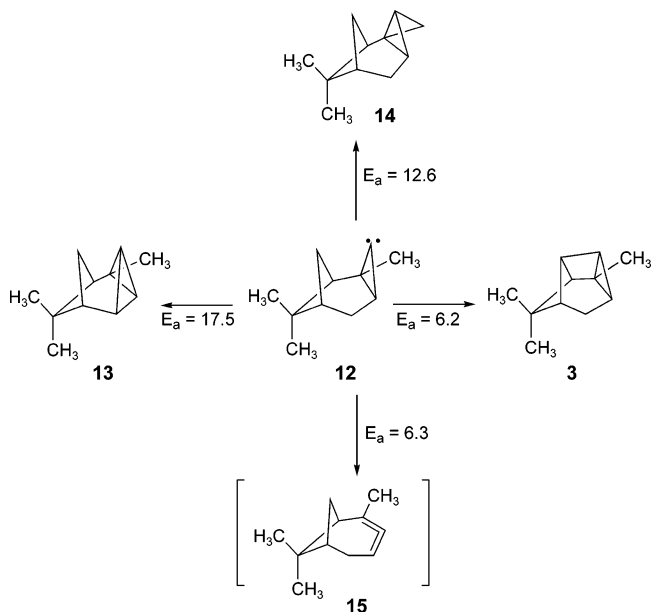
Computational Methods

The GAUSSIAN 98W¹³ program was used for density functional theory calculations, employing Becke's three-hybrid method and the exchange functional of Lee, Yang, Parr (B3LYP). The geometry optimizations of all the structures were achieved at the B3LYP/6-31G(d) level. Energies were refined by using B3LYP/6-31G(d) single-point evaluations. Stationary points were characterized as minima or transition

TABLE 1. The Relative Energy Values (kcal/mol) for Products of the Ring Opening of Bicyclo[4.1.0]hept-7-ylidene (**8**) Calculated by Using the B3LYP/6-31G(d) Basis Set and Their Literature Values

	rel energy	
	B3LYP/6-31G(d)	B3LYP/TZP ¹²
9	6.2	6.4
10	9.6	9.1
11	15.1	14.6

SCHEME 3



structures by way of an analytic evaluation of harmonic vibrational frequencies at the level of geometry optimization.

Results and Discussions

To analyze the reliability of the 6-31G(d) basis set with respect to the TZP basis set, which was used for the reactions of bicyclo[4.1.0]hept-7-ylidene (**8**),¹² the B3LYP geometry optimizations were performed again at the chosen basis set. Single-point energies were evaluated at this level. As can be seen in Table 1, our results are found to be consistent with reported literature values.

After this we turned our attention to elucidate the insertion and ring-opening reactions of carbenoid **12**.¹⁴ Three possible products can be considered for the intramolecular CH-insertion reactions of **12**: 3,7,7-trimethyltetracyclo[4.2.0.0^{2,4}.0^{3,8}]octane (**3**), 2,7,7-trimethyltetracyclo[4.1.1.0^{2,4}.0^{3,5}]octane (**13**), and 8,8-dimethyltetracyclo[5.1.1.0^{2,4}.0^{2,5}]nonane (**14**) (Scheme 3). The computed activation energy barriers (kcal mol⁻¹) for their internal CH-insertions are predicted to be 6.2 (TS1) for **12** → **3**, 12.6 (TS2) for **12** → **14**, and 17.5 (TS3) for **12** → **13** (Figure 1 and Table 2). According to these results, the formation of insertion products, **13** and **14**, is less likely, whereas **3** can be easily formed during the reaction. On the other hand, the activation barrier for the disrotatory ring-opening reaction forming allene, **12** → **15**, is predicted

(10) (a) Moore, W. R.; Ward, H. R.; Merritt, R. F. *J. Am. Chem. Soc.* **1961**, *83*, 2019–2020. (b) Köbrich, G.; Goyert, W. *Tetrahedron* **1968**, *24*, 4327–4342.

(11) Paquette, L. A.; Taylor, R. T. *J. Am. Chem. Soc.* **1977**, *99*, 5708–5715.

(12) Bettinger, H. F.; Schleyer, P. v. R.; Schreiner, P. R.; Schaefer, H. F., III. *J. Org. Chem.* **1997**, *62*, 9267–9275.

(13) Frisch, M. J.; Trucks, G. W.; Schlegel, H. B.; Scuseria, G. E.; Robb, M. A.; Cheeseman, J. R.; Zakrzewski, V. G.; Montgomery, Jr., J. A.; Stratmann, R. E.; Burant, J. C.; Dapprich, S.; Millam, J. M.; Daniels, A. D.; Kudin, K. N.; Strain, M. C.; Farkas, O.; Tomasi, J.; Barone, V.; Cossi, M.; Cammi, R.; Mennucci, B.; Pomelli, C.; Adamo, C.; Clifford, S.; Ochterski, J.; Petersson, G. A.; Ayala, P. Y.; Cui, Q.; Morokuma, K.; Malick, D. K.; Rabuck, A. D.; Raghavachari, K.; Foresman, J. B.; Cioslowski, J.; Ortiz, J. V.; Baboul, A. G.; Stefanov, B. B.; Liu, G.; Liashenko, A.; Piskorz, P.; Komaromi, I.; Gomperts, R.; Martin, R. L.; Fox, D. J.; Keith, T.; Al-Laham, M. A.; Peng, C. Y.; Nanayakkara, A.; Challacombe, M.; Gill, P. M. W.; Johnson, B.; Chen, W.; Wong, M. W.; Andres, J. L.; Gonzalez, C.; Head-Gordon, M.; Replogle, E. S.; Pople, J. A. *Gaussian 98*, Revision A.8; Gaussian, Inc., Pittsburgh, PA, 1998.

(14) For the chemistry of cyclopropylidenes see: Backes, J.; Brinker, U. H. In *Houben-Weyl (Methoden der Organischen Chemie)*; Regitz, M., Ed.; Thieme: Stuttgart, Germany, 1989; Vol. E 19b, pp 391–510.

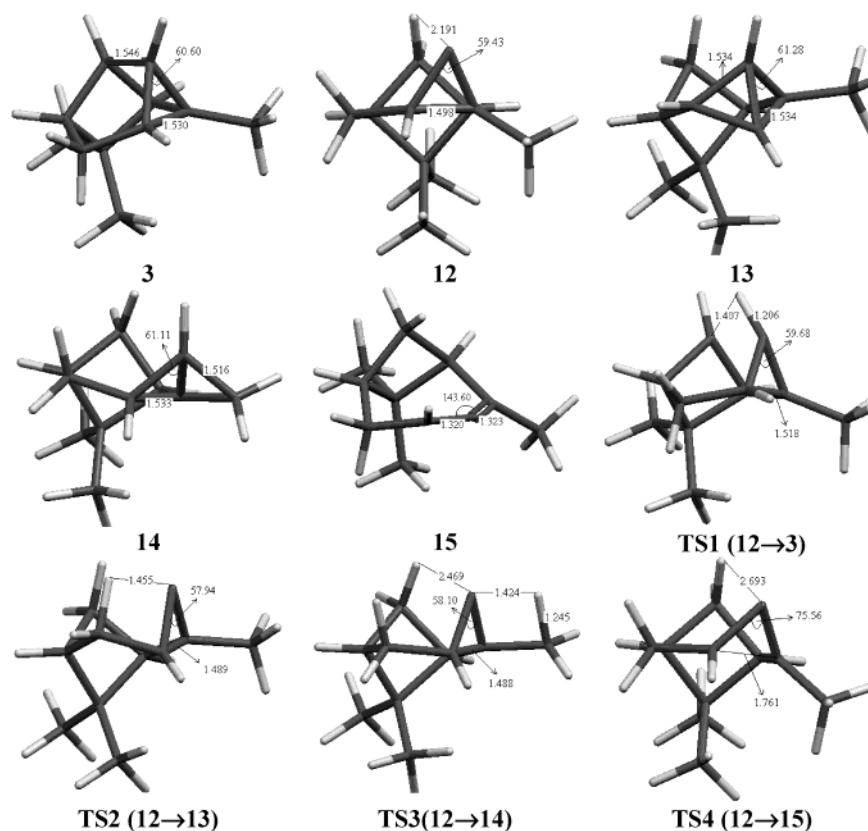


FIGURE 1. Optimized structures of **3**, **12**, **13**, **14**, and **15** and transition structures **TS1**, **TS2**, **TS3**, and **TS4** at B3LYP/6-31G(d).

SCHEME 4

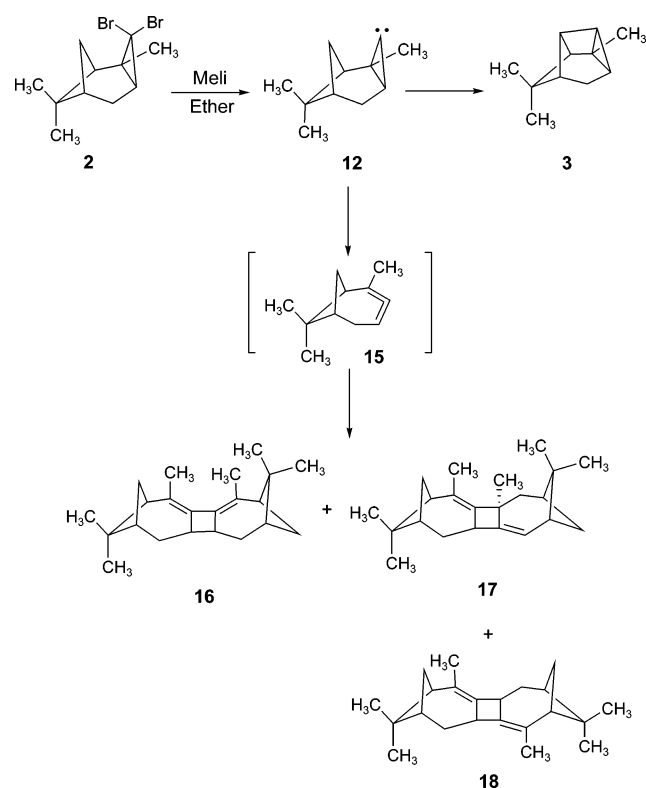


TABLE 2. Absolute Energies (E , in hartree/particle), Number of Imaginary Frequencies [in brackets], Zero-Point Vibrational Energies (ZPVE, in kcal/mol), and Energies Relative to the Carbene Ground State Including Zero-Point Corrections (in kcal/mol) for the Insertion Products **3**, **13**, **14**, and **15** and Related Transition States

	energy	ZPVE	rel energy
12	−428.61424 [0]	150.4	0.0
3	−428.71827 [0]	152.3	−63.3
13	−428.67802 [0]	151.7	−38.7
14	−428.69134 [0]	152.7	−46.0
15	−428.69093 [0]	151.5	−46.9
TS1(12→3)	−428.60140 [1]	148.6	6.2
TS2(12→13)	−428.58417 [1]	149.0	17.5
TS3(12→14)	−428.59236 [1]	149.2	12.6
TS4(12→15)	−428.60370 [1]	150.1	6.3

the reaction of **2** with MeLi is carried out at either low or high temperatures.

To test the validity of these theoretical calculations we have repeated the reaction of dibromocyclopropane **2** with MeLi at various temperatures. First, we synthesized 3,3-dibromo-2,7,7-trimethyl-tricyclo[4.1.1.0^{2,4}]octane (**2**)¹⁵ from α -pinene via dibromocyclopropane addition by treatment with bromoform and potassium *tert*-butoxide in hexane. The obtained dibromocyclopropane **2** was reacted with MeLi in dry ether at various temperatures. After the usual aqueous workup procedure and vacuum distillation

to be 6.3 kcal mol^{−1}, which is as low as that of the insertion reaction **12** → **3**. This explains that both allene product **15** and insertion product **3** can be isolated when

(15) (a) Hatem, J.; Waegell, B. *Tetrahedron* **1990**, *46*, 2789–2806. (b) Hatem, J.; Waegell, B. *Tetrahedron Lett.* **1973**, *23*, 2023–2026. (c) Graefe, J.; Thank, L. M.; Muehlstaedt, M. *Z. Chem.* **1971**, *11*, 252–253.

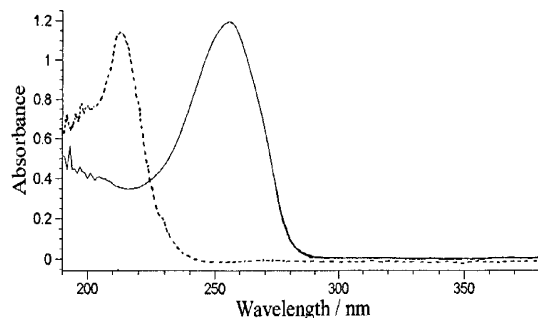


FIGURE 2. UV spectra for the dimeric products in hexane (**16**: solid line, 9.41×10^{-5} M, $\lambda_{\max} = 260$ nm, $\epsilon = 12698$ M $^{-1}$ cm $^{-1}$; **17** + **18**: dashed line, 7.63×10^{-5} M, $\lambda_{\max} = 212$ nm, $\epsilon = 15068$ M $^{-1}$ cm $^{-1}$).

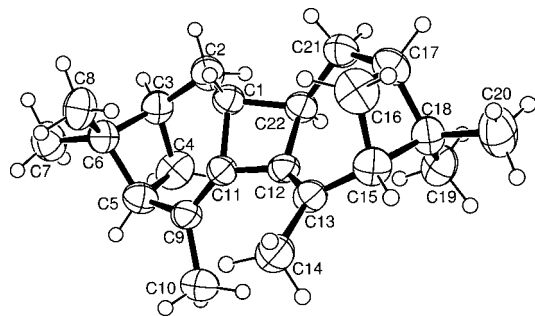


FIGURE 3. X-ray crystal structure of the allene dimer **16**.

for the separation of the insertion product **3**, the residue was analyzed by ^1H and ^{13}C NMR measurements, whose spectra showed the formation of three dimeric products, **16**, **17**, and **18**, with a total yield of 37%.

Column chromatography on SiO_2 and subsequent recrystallization from ethanol afforded **16** as colorless crystals, whose UV spectrum in hexane showed absorption bands at 260 nm (Figure 2). This value indicates the existence of a conjugated butadiene structure.^{3a}

Furthermore, an 11-line ^{13}C NMR spectrum and the molecular peak of 296 (M^+) clearly indicated the presence of an allene dimer. Moreover, X-ray analysis of **16** was carried out to determine its exact configuration. As can be seen from Figure 3, it is a head-to-head dimer and the dimethyl bridges are in the anti position.

All efforts with column chromatography, crystallization, and distillation to separate the diastereomeric mixture consisting of **17** and **18** in a ratio of 1:1 (determined by ^1H NMR spectroscopy) failed. The UV spectrum of this mixture showed an absorption band at $\lambda = 212$ nm and no distinct peaks around 260 nm. This observation indicates that both diastereomeric isomers have a nonconjugated butadiene unit. Furthermore, a 31-line ^{13}C NMR (two lines are overlapped, a total sum of 33 lines) spectrum showed the presence of a symmetrical and an unsymmetrical dimerization products. Furthermore, the presence of a vinyl proton resonating as a doublet at 5.18 ppm indicated the presence of a head-to-tail dimerization product **17**. The mass spectrum of the mixture showed a single peak at 296 (M^+), which is equal to the molecular weight of dimer. The elemental analysis of the mixture was also in agreement with that of the expected structures.

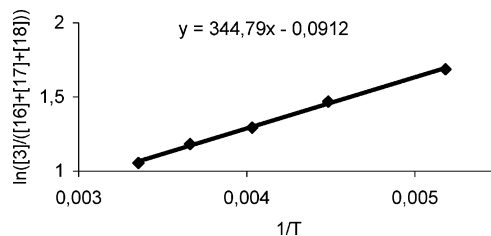


FIGURE 4. A graph of $\ln([3]/([16] + [17] + [18]))$ versus $1/T$ (K^{-1}).

TABLE 3. The Amount of Products (in mol unit) for the Reaction between 3,3-Dibromo-2,7,7-trimethyltricyclo[4.1.1.0^{2,4}]octane (**2**) and MeLi at Different Temperatures

temp ($^{\circ}\text{C}$)	[3]	[16] + [17] + [18]	[3]/([16] + [17] + [18])
-80	0.0319	0.00590	5.407
-50	0.0301	0.00693	4.343
-25	0.0294	0.00807	3.643
0	0.0281	0.00863	3.256
25	0.0273	0.00951	2.871

Additionally, the amount of products at different temperatures was investigated for the reaction of **2** with MeLi. As is seen in Table 3, the amount of dimerization products increased at the cost of that of the insertion product **3** when the reaction temperature increased from -80 $^{\circ}\text{C}$ up to 25 $^{\circ}\text{C}$. The steady-state approximation can be applied on the allene intermediate **15**. If this is done, the following product ratio can be found

$$\frac{[\mathbf{3}]}{[\mathbf{16}] + [\mathbf{17}] + [\mathbf{18}]} = \frac{k_1}{k_2}$$

where k_1 is the rate constant for the appearance of **3** and k_2 is the rate constant for the formation of allene **15**. From this equation the trend of increasing product ratio in favor of **3** as the temperature is decreased is shown by a plot of $\ln([3]/([16] + [17] + [18]))$ versus $1/T$ (Figure 4). This shows that the energy barrier for the k_2 step leading to allene **15** is larger than that for the k_1 step leading to **3**. According to the Arrhenius equation, the difference in activation energy between two products **3** and **15** can be calculated from the slope of this graph as 0.685 kcal. These results are in agreement with our theoretical results

Experimental Section

3,3-Dibromo-2,7,7-trimethyltricyclo[4.1.1.0^{2,4}]octane (2**).**¹⁴ A solution of 69 g (0.5 mol) of 1*R*(+)- α -pinene in 100 mL of hexane was added to a mechanically stirred suspension of potassium *tert*-butoxide (65.1 g, 0.58 mol) in hexane (500 mL), which was then pre-cooled and maintained at -10 $^{\circ}\text{C}$ under a nitrogen atmosphere. A solution of bromoform (131.4 g, 0.52 mol) in hexane (100 mL) was then introduced to this suspension over 4 h while maintaining the reaction mixture at -10 $^{\circ}\text{C}$. After the addition was completed, the mixture was stirred at room temperature for 4 h and hydrolyzed through the addition of water (200 mL). The organic layer was washed with a saturated NaCl solution (200 mL) and dried over MgSO_4 . After the removal of the solvent, the residue was crystallized from hexane to provide cyclopropane adduct **2** as colorless crystals (109 g, 71%): mp 67.2 – 68.7 $^{\circ}\text{C}$; ^1H NMR (400 MHz, CDCl_3) δ 2.41 (d, $J = 11.5$ Hz, 1H), 2.06–2.13 (m, 1H), 1.96 (t, $J = 5.5$ Hz, 1H), 1.76 (ddd, $J = 11.4, 5.5, 2.1$ Hz, 1H), 1.70 (d, $J = 14.7$ Hz, 1H), 1.54 (m, 1H), 1.49–1.53 (m, 2H),

1.16 (s, 3H), 1.29 (s, 3H), 0.84 (s, 3H); ^{13}C NMR (100 MHz, CDCl_3) δ 50.8, 48.6, 43.4, 39.9, 35.0, 32.6, 27.1, 26.8, 26.7, 26.2, 22.5; IR (KBr, cm^{-1}) 2975, 2907, 1447, 1368, 1274, 1222, 1177, 1109, 1011, 942, 892, 836. Anal. Calcd for $\text{C}_{11}\text{H}_{16}\text{Br}_2$: C, 42.89; H, 5.24. Found: C, 42.73; H, 5.08.

Reaction of 3,3-Dibromo-2,7,7-trimethyl-tricyclo[4.1.1.0^{2,4}]octane (2) with MeLi. To a solution of **2** (15.40 g, 50.0 mmol) in dry ether (100 mL) was added dropwise 1.6 M MeLi in ether (37.5 mL, 60 mmol) at room temperature and the resulting solution was stirred for 2 h. The reaction mixture was quenched with water. The mixture was extracted with ether, and the organic layer was washed with saturated NaCl and dried over MgSO_4 . After the removal of the solvent (20 °C, 15 Torr), the product mixture (8.77 g) was distilled at 38 °C (5 Torr) to provide the insertion product **3,7,7-trimethyltetracyclo[4.2.0.0^{2,4}.0^{3,8}]octane (3)**⁸ (4.04 g, 54%): colorless liquid; ^1H NMR (400 MHz, CDCl_3) δ 2.57 (ddd, J = 11.8, 4.6, 3.4 Hz, 1H), 2.02 (d, J = 12.0 Hz, 1H), 1.94 (dd, J = 10.6, 4.8 Hz, 1H), 1.89 (dd, J = 10.1, 4.6 Hz, 1H), 1.72 (t, J = 3.5 Hz, 1H), 1.66 (dd, J = 11.8, 6.9 Hz, 1H), 1.20 (d, J = 4.2 Hz, 1H), 0.99 (s, 3H), 0.74 (s, 3H), 0.60 (s, 3H); ^{13}C NMR (CDCl_3 , 100 MHz) δ 49.0, 48.0, 36.8, 35.7, 32.0, 31.3, 27.5, 27.1, 26.0, 20.4, 19.5; IR (NaCl, cm^{-1}) 2998, 2936, 2861, 1454, 1364, 1267, 1147, 1125, 918, 865, 778; MS m/z 148 (M^+ , 23%), 133 (100), 115 (37), 105 (100), 91 (100), 77 (98), 69 (100), 65 (61), 51 (56), 42 (34). Anal. Calcd for $\text{C}_{11}\text{H}_{16}$: C, 89.12; H, 10.88. Found: C, 89.02, H, 10.91.

The residue was passed through silica gel (70 g) eluting with hexane to yield head-to-head allene dimer **1R,6R,8S,10R,11R,13S-2,5,7,7,14,14-hexamethylpentacyclo[11.1.1.1^{6,8}.0^{3,11}.0^{4,10}]hexadeca-2,4-diene (16)**. Recrystallization from ethanol provided pure **16** as colorless crystals (1.62 g, 22%): mp 122.5–123.0 °C; ^1H NMR (400 MHz, CDCl_3) δ 2.80 (q, J = 9.0 Hz, 2H), 2.72 (m, 2H), 2.28–2.15 (m, 6H), 1.81 (s, 6H), 1.66 (dd, J = 13.8, 4.6 Hz, 2H), 1.37 (s, 6H), 1.25 (d, J = 10.5 Hz, 2H), 1.12 (s, 6H); ^{13}C NMR (100 MHz, CDCl_3) δ 136.0 (C), 127.7 (C), 52.4 (CH), 51.4 (CH), 44.1 (CH), 42.0 (C), 38.5 (CH_2), 34.4 (CH_2), 32.3 (CH_3), 30.1 (CH_3), 22.9 (CH_3); IR (KBr) 2960, 2912, 2858, 1448, 1363, 1273, 1235, 1220, 1038, 918, 778 cm^{-1} ; MS m/z 296 (M^+ , 12%), 255 (12), 227 (17), 197 (6), 183 (11), 171 (17), 157 (26), 143 (27), 128 (30), 115(20), 105(26), 91 (44), 77

(31), 69 (72), 55 (36), 41 (100). Anal. Calcd for $\text{C}_{22}\text{H}_{32}$: C, 89.12; H, 10.88. Found: C, 88.91; H, 10.83. The UV spectrum in hexane is shown in Figure 1.

The second fraction was the oil of a diastereomeric mixture of head-to-tail dimer **7,7,9,11,14,14-hexamethylpentacyclo[11.1.1.1^{6,8}.0^{3,11}.0^{4,10}]hexadeca-2,9-diene (17)** and head-to-head allene dimer **2,7,7,9,14,14-hexamethylpentacyclo[11.1.1.1^{6,8}.0^{3,11}.0^{4,10}]hexadeca-2,9-diene (18)** (1.19 g, 15%): IR (NaCl) 2963, 2902, 1450, 1382, 1364, 1227, 1129, 1068, 844, 825 cm^{-1} ; ^1H NMR (400 MHz, CDCl_3) δ 5.19 (d, J = 7.6 Hz, 1H), 2.68 (br s, 1H), 2.61 (t, J = 7.8 Hz, 1H), 2.3–2.15 (m, 3H), 2.05–1.75 (m, 7H), 1.61–1.65 (m, 2H), 1.51 (s, 3H), 1.24–1.32 (m, 1H), 1.12 (s, 3H), 1.10 (s, 3H), 0.89 (s, 3H), 0.75 (s, 3H), 0.67 (s, 3H); the ^{13}C NMR data for isomers **17** and **18** were extracted from the NMR mixture with the help of COSY, HMQC, HMBC, and DEPT spectra. **18**: 137.0 (C), 127.0 (C), 52.0 (CH), 47.7 (CH), 42.5 (2 \times CH), 31.5 (CH_2), 30.9 (CH_3), 25.6 (CH_2), 23.3 (CH_3), 21.0 (CH_3). ^{13}C NMR data for **17**: 146.7 (C), 140.1 (C), 126.2 (C), 116.4 (CH), 51.98 (C), 51.5 (CH), 49.5 (CH), 44.7 (CH), 43.9 (C), 43.2 (C), 42.8 (CH), 42.5 (CH), 41.4 (C), 32.2 (CH_3), 30.1 (CH_2), 26.4 (CH_2), 25.3 (CH_3), 24.2 (CH_2), 23.8 (CH_2), 21.2 (CH_3), 21.0 (2 \times CH_3), 20.14 (CH_3). **17** and **18**: MS m/z 296 (M^+ , 12%), 255 (13), 227 (22), 183 (18), 169 (22), 157 (36), 128 (53), 91 (78), 69 (89), 41 (100). Anal. Calcd for $\text{C}_{22}\text{H}_{32}$: C, 89.12; H, 10.88. Found: C, 88.85; H, 10.79. The UV spectrum of the mixture in hexane is shown in Figure 1.

Acknowledgment. The authors are indebted to the Scientific and Technical Research Council of Turkey (Grant TUBITAK-MISAG-216) and the Turkish Academy of Sciences for their financial support. Furthermore, we are grateful to the referees for their helpful suggestions.

Supporting Information Available: X-ray data for **16** as a CIF file and Cartesian coordinates for **3**, **12**, **13**, **14**, and **15** and **TS1**, **TS2**, **TS3**, and **TS4** optimized at the B3LYP/6-31(d) level. This material is available free of charge via the Internet at <http://pubs.acs.org>.

JO035450Z